Rheology and morphology of multilayer reactive polymers: effect of interfacial area in interdiffusion/reaction phenomena

Khalid Dr. Lamnawar, Abderrahim Maazouz

Rheology and morphology of multilayer reactive polymers: effect of interfacial area in interdiffusion/reaction phenomena

Khalid Lamnawar, **Abderrahim Maazouz**

Abstract The rheological behavior of multilayered reactive polymers was investigated. Dynamic mechanical experiments were performed to probe the effect of the interfacial area on the rheological behavior of a multilayered structure as compared to that of a droplet-type morphology. Polyamide (PA6)/polyethylene grafted with glycidyl methacrylate was used as a model system, and in the molten state, such a system generated a reaction between amine, carboxylic, and epoxy groups. Multilayer structures containing various amounts of both interfacial area and volume fractions of the two components were studied. Relationships between viscoelastic material functions and compositions were used to analyze the effects of bulk and reactive functions in the polyolefin phase at the interface with PA. The contribution of the interface/interphase effect was investigated along with the increase in the number of layers, and the results showed that the variation in dynamic modulus of the multilayer system was a result of both diffusion and chemical reaction. Specific experiments were carried out to separate the thermodynamic effects from the kinetic ones, and the results were rationalized by comparing the obtained data with theoretical models. Finally, the effect of the interface/interphase triggered between the neighboring layers was quantified at a specific welding time and shear rate.

K. Lamnawar · A. Maazouz (✉)
Ingénierie des Matériaux Polymères Laboratoire des Matériaux Macromoléculaires (IMP/LMM), UMR-CNRS 5223, INSA-Lyon, Université de Lyon,
69621 17 Avenue Jean Capelle,
Villeurbanne Cedex, France
e-mail: Abderrahim.maazouz@insa-lyon.fr

K. Lamnawar
e-mail: Khalid.Lamnawar@insa-lyon.fr

A. Maazouz
Hassan II Academy of Sciences and Technologies,
Rabat, Morocco

Keywords Rheology at the interface · Interfacial reaction · Interdiffusion · Coextrusion · Interfacial area · Multilayer polymers · Interphase · Blends

Introduction

In our previous work (Lamnawar and Maazouz 2006), we have used rheometry as a tool for probing the competition between interdiffusion and reaction at a polymer/polymer interface in a bilayer sandwich structure. The results provided an upstream study for optimizing the processing of layered plastic composites of reactive polymer systems with synergistic final properties of the elaborated materials. Such systems are therefore potential candidates for packaging applications.

Another unique feature of a multilayer structure is its large amount of specific interfacial area generated in a well-controlled manner. This makes it an excellent model system for studying interfacial phenomena in polymer blends. As polymers are often immiscible, various morphologies may occur during melt mixing (Prochazka et al. (2004)). Droplet/matrix, fibrillar, lamellar, or co-continuous morphologies have been observed. Each of these morphologies depends on several factors such as composition, processing conditions (e.g., mixing time, temperature, shear, and elongational rate) or the nature of the polymers (e.g., interfacial tension, viscosity, and elasticity) (Utracki 2000). During the last decade, important theoretical and experimental advances on the rheology of liquid mixtures and polymer blends have been accomplished. Some of the recent developments may be found in the review article of Tucker and Moldenaers (2002). Yu et al. (2002) have also published some interesting results offering a better understanding and have proposed a generic model providing a direct coupling between flow,

structure, and stress. Furthermore, it is possible to extract morphological information from rheological material functions of a polymer blend and vice versa. However, most of these studies were carried out in melt blended systems where mixing and interfacial area generations were a function of interfacial properties and rheology. Moreover, these two properties have been found to interact in the blending process.

The apparent kinetics of an interfacial reaction include a combination of diffusion of functional groups to the interfaces and reaction at the interfaces. The limiting step can vary not only for different systems but also in the same system at different stages in the blending process. Theoretical studies (Fredrickson and Scott Milner 1996; O'Shaughnessy and Vavylonis 1999) suggest three regimes for the kinetics of interfacial reactions: (1) the reaction rate is controlled by the quasi-local reaction rate near the interface; (2) the reaction rate is controlled by the center of mass diffusion of the reactive homopolymer to the interface; and (3) the reaction rate is controlled by the diffusion barrier presented by the growing copolymer layer.

Recently, some experimental studies of the interfacial reaction kinetics and properties by the planar model have been reported in the literature. The work by Harton et al. (2005) showed that the coupling reaction of PS-OH/PMMA-co-MAC was diffusion-controlled. The study by Schulze et al. (2000) demonstrated that the coupling reaction of PS-NH2/PMMA-anh was reaction-controlled. These results indicated that the in situ copolymer formation was limited by the reaction rate, rather than by the diffusion of reactive chains through the bulk.

On the other hand, many studies have focused on investigating the effect of reaction kinetics on the interfacial morphology of reactive bilayer systems using transmission electron microscopy (TEM) and atomic force microscopy (AFM; Jiao et al. 1999; Lyu et al. 1999; Kim et al. 2005; Zhang et al. 2005). With AFM, a solvent was used to remove the top layer, and the revealed surface was found to have become roughened as a function of reaction time. With TEM, the cross-section of the interface was examined, and an emulsified region was observed at the interface.

Kim et al. (2003, 2006) investigated the interfacial reaction kinetics for PS-mCOOH/PMMA-GMA and proposed three distinct stages for the changes in the viscosity modulus with time. They also investigated the change in the interfacial morphology by AFM and TEM and found that for this system, microemulsions were formed in the bulk phase. However, they did not give a very clear physical explanation for the correlation of the change in rheological properties with the conversion of the in situ formed copolymers.

Indeed, it should be noted that the interfacial morphology of a reactive bilayer system depends on the reaction kinetics of two reactive polymers, the position of the functional group in a reactive polymer chain, and the molecular weight of the polymers (Xiaobo et al. 2005; Fan et al. 2005).

In reactive blending, functional groups from two polymers connect either end-to-end, leading to the formation of block copolymers at the interfaces between the two immiscible polymers (Baker et al. 2001). These block copolymers facilitate the mixing of the two phases and stabilize the microphases in the blends. Many studies have been performed to understand the fundamentals of reactive compatibilization; however, the kinetics of interfacial reactions are still not understood. Difficulties arise from the fact that reactions take place at the polymer–polymer melt interfaces. Nevertheless, the interfacial morphology is not well controlled, and the interfacial area cannot be quantified in the blending process.

The problems here consist in: (1) the interfacial area changing during the blending and (2) the rheological properties of the blends changing with respect to the extent of the interfacial reaction. As a consequence, the interfacial reaction and interfacial area generation are coupled in reactive blending. Because of this, most of the reported data of the reaction kinetics is based on the total volume of the blends. It is thus not a direct measurement of the interfacial reaction but rather a combination of many aspects in blending. This data often contains ambiguity and causes confusion when applied to other systems, and it has a limited value in the understanding of the fundamentals behind reactive blending.

A model system separating the interfacial reaction from the interfacial area generation is needed to be able to clearly study the competition between interdiffusion and reaction phenomena. This renders it difficult to clearly separate these two aspects and investigate their individual roles in morphology development. In contrast, the morphology in a multilayer system is well defined by the number of layers and their thicknesses. The interfacial area generation is not determined by interfacial properties and rheology up to the point where the layers break up. The large number of layers, which gives a large amount of specific interfacial area, greatly magnifies a small change in the interface and produces macroscopically measurable quantities. This makes it a suitable model system for studying interfacial dynamics in polymer blending.

The present investigation deals with dynamic mechanical experiments that were used to probe the effect of the interfacial area on the rheological behavior of a multilayered structure. This was then compared to a droplet-type morphology of an equivalent blend. The systems chosen for the study were polyethylene-grafted with glycidyl methacrylate (PE-GMA)/PA6 as the reactive system and PE/PA6 as the nonreactive one. A reaction between amine, carboxylic, and epoxy groups is generated in the molten state for this type of reactive system.

Experimental section

Materials

The main characteristics of the materials used in this study are reported in Table 1. The functionalized nylon (PA6) was terminated with primary amino and carboxylic groups. The PE was grafted with a random copolymer of ethylene and 8 wt% (0.56 mol/kg) of glycidyl methacrylate (PE-GMA). It had approximately 10.5 functional units per chain on the basis of the average molecular weight. Carboxylic and amino groups were situated only at the ends of PA and could react with the epoxy groups in PE-GMA as illustrated in our previous work (Lamnawar and Maazouz 2006). The advantages of using GMA functionalization include the faster grafting reaction onto polyolefins, when compared to that of maleic anhydride or acrylic acid. Moreover, the bulky structure of GMA is believed to reduce cross-linking and chain scission within the polymer backbone (Wei et al. 2005). Another important aspect is that the formation of water does not occur during the reaction of the epoxide ring with –COOH or $–NH_2$ groups of PA in the melt, thus preventing the hydrolysis of chain bonds formed at the interface. In the present paper, the PE-GMA/PA6 was referred to as RS (reactive sandwich) and PE/PA6 as NRS (nonreactive sandwich).

Rheology of multilayer systems

Multilayer samples were fabricated on a coextrusion line in our laboratory into 360-mm-wide films. Initially, the polymers were brought together in a feed block, which arranged them into multiple alternating layers. Not to obstruct the clarity of this paper, further details concerning this specific setup are described elsewhere (Lamnawar and Maazouz 2007a).

Two multilayer structures, prepared by a coextrusion process (T=230 °C, residence time=70 s for all structures (Lamnawar and Maazouz 2007a), were studied: one containing varying amounts of interfacial surface but a constant volume fraction of the two components and the other containing varying volume fractions of the components, but with a constant amount of interfacial surface between them. To form multilayer films, individual films were placed on top of one another at room temperature. Compositions of 30, 50, and 70 vol% of PE were prepared, while the surface between the two materials was kept constant. Multilayer films with a composition of 50 and 70 vol%, but with varying amounts of interfacial surface, were also prepared.

All film samples were fabricated under identical processing conditions to eliminate sample-to-sample errors. The obtained samples were then cut into disks with diameters of 25 mm. Subsequently, these round film samples were annealed at 40 °C under vacuum for 1 week to remove possible surface contaminants and to allow the relaxation of chains at the surface that had become oriented during the coextrusion as a result of shear and elongation.

The rheological experiments of the neat components and of the multiphase systems were performed with a strain-controlled rheometer: Advanced Rheometrics Expansion System (ARES, Rheometrics) using a parallel-plate geometry (Φ=25 mm). Sample discs were placed between the plates and melted. In this study, zero time was defined as the time when the heating chamber of the rheometer was closed, and the healing time was the contact time after having reached the plate temperature. Polymer degradation was avoided by continuously purging the oven with nitrogen. Such a manipulation had to be fast and carefully executed to avoid a rapid decrease of the plate temperature, and the temperature control was considered satisfactory within a range of ±0.5 °C. The polymer sandwich was slightly compressed to obtain a gap between the plates of no more than 1.18 mm. Indeed, the pressure was expected to affect the diffusion process and thus also the interpenetration of chains at the interface.

Measurements were taken once the sample had reached a fully relaxed state, which was indicated by a normal force of less than 10%. Frequency and dynamic time sweep experiments were carried out with a maximum strain level (γ_0) of 5% and an angular frequency range of 0.05–100 rad/s, thus assuring that the measurements were carried out in the linear viscoelastic regime. All measurements, whether of RS or NRS, were performed with a 200 FRTN1 transducer with a lower limit of 0.02 g·cm.

Table 1 Material characteristics

Sample code	Trademark/Supplier	Reactive groups	M_w	M_w/M_n^a	Melting temperature	Ea (Kj/mol)
PE	Lacqtene/ARKEMA	Nonreactive	207,000	9.9	114	53
PE-GMA	LotaderAX8840/ARKEMA	Epoxy functions	240,000	10.2	107	56
PA6	Capron/BASF	Primary amino and carboxylic ends of chains	34,000	2	224	45

Mixing step for rheological and morphological measurements

The equivalent blends of multilayer systems at two composition ratios, i.e., 50/50 and 70/30 wt%, were prepared in a PRISM PTW 16/25 D co-rotating twin screw extruder with a screw diameter of 16 mm (Thermo Electron Polylab System-Rheocord RC400p). The mixing procedure involved two strategies for the preparation of in situ PE-GMA/PA blends. These consisted in dispersing PA6 in two forms:

1. PA6, in its molten state, was dispersed in the PE-GMA matrix (emulsion type mixture). The high modulus polymer [with a melting temperature (T_d) of 220 °C] and the thermoplastic matrix [with a melting temperature (T_M) 120 °C lower than T_d] were thus blended in a twin screw extruder at a temperature $T_1 > T_d$, T_M, i.e., both phases were in the molten state.
2. PA6 was dispersed as a filler in the PE-GMA matrix (suspension type mixture). In this case, the extrudate was prepared at a temperature of 180 °C at which the dispersed PA6 phase was solid and the matrix was molten.

The flow rate was 0.3 kg/h and the screw speed was 100 rpm. The following temperatures were chosen for the five heating zones from hopper to die, where the last value corresponds to the die temperature:

(a) 170–170–170–170–183 °C
(b) 170–220–228–230–240 °C

Table 2 lists the composition of all examined blends and includes the screw speeds and die temperatures. The reactive blends were random copolymers of ethylene and 8 wt% (0.56 mol/kg) of glycidyl methacrylate and were denoted PE-GMA. They had approximately 10.5 functional units per chain on the basis of the average molecular weight, i.e., BSR50 or BSR70, which was dependent on the percentage of PE-GMA. The denotations E and S corresponded to an emulsion and suspension mixture, respectively. For instance, a sample denoted E240r100 refers to an emulsion mixture prepared with a die temperature of 240 °C and a screw speed of 100 rpm.

The extrudate was quenched in a cold water bath and subsequently granulated. The obtained blend granules were carefully dried under vacuum at 80 °C for 12 h and then molded into samples with 25 mm diameters and 1 mm thicknesses for rheological measurements.

Table 2 Blends prepared with the PRISM 16 mm extruder to be compared with the multilayer systems

BSR50	BSR70
S183r100	S183r100
E240r100	E240r100

Electron microscopy and image analysis

The samples were fractured in liquid nitrogen, and the morphology of the blend was examined by scanning electron microscopy (Environmental SEM Hitachi S-3500N). Cross-sections parallel and perpendicular to the flow directions were systematically considered, but as in all circumstances, spherical droplets were observed, only the transverse cross-sections were ultimately analyzed. A minimum of five micrographs were obtained for each sample, and approximately 200 particles were considered to determine the droplet diameter of the dispersed phase using an image analysis software (Scion image). The number $(\overline{D_n})$ and weight $(\overline{D_w})$ average diameters were determined using the following equations:

The number average diameter : (1)

$$\overline{D}_n = \frac{\sum_i n_i \overline{D}_i}{\sum_i n_i}$$

The weight − average diameter : (2)

$$\overline{D}_w = \frac{\sum_i n_i \overline{D}_i^2}{\sum_i n_i \overline{D}_i}$$

From the dispersed droplet type morphology, the parameter for the interfacial area per unit volume (Ai; Thomas and Groeninckx 1999) was calculated according to:

$$A_i = \frac{3\phi}{R} \quad (3)$$

In this equation, ϕ is the volume fraction of the dispersed phase and R the radius of the dispersed particles, respectively.

This is a very simple equation that has been largely used by others and can be easily found (the total surface area per unit volume is $S_v = \frac{N4\pi R^2}{V}$ where V is the total volume and N the number of drops. From the volume fraction per unit volume, i.e., $\phi = \frac{N(4/3)\pi R^3}{V}$, one can extract the volume, and its insertion in the above equation gives Eq. 3).

Results and discussion

Viscoelastic properties of bilayer systems and their equivalent blends

For reactive multilayer systems, graft (or block) copolymers formed in situ at the interface are able to give rise to changes in the complex viscosity. Rheological methods can be used

to monitor the interfacial reaction. Figure 1 portrays the viscosity vs the angular frequency at 240 °C for (a) a reactive PE-GMA/PA6 bilayer system (with 50 vol% PA6) and its respective neat components and (b) a non reactive PE/PA6 bilayer system (with 50 vol% PA6) and its respective neat components. Indeed, the flow curve (Fig. 1a) of PE-GMA/PA6 (RS) showed a sharp increase in viscosity at low frequencies (yield). However, this phenomenon was not present in the case of the pure polymers. In fact, $\eta^*(\omega)$ for the NRS was also plotted on the same graph (Fig. 1b), and as can be seen, no significant increase in viscosity was found, thus confirming that the phenomenon observed was caused by the reactivity at the interface at low shear rates. There was thus a clear distinction between the two systems.

Meanwhile, the increase in $\eta^*(\omega)$ was evidence of the copolymer formation from the reaction of PE-GMA and the carboxylic and amine end functions of PA6.

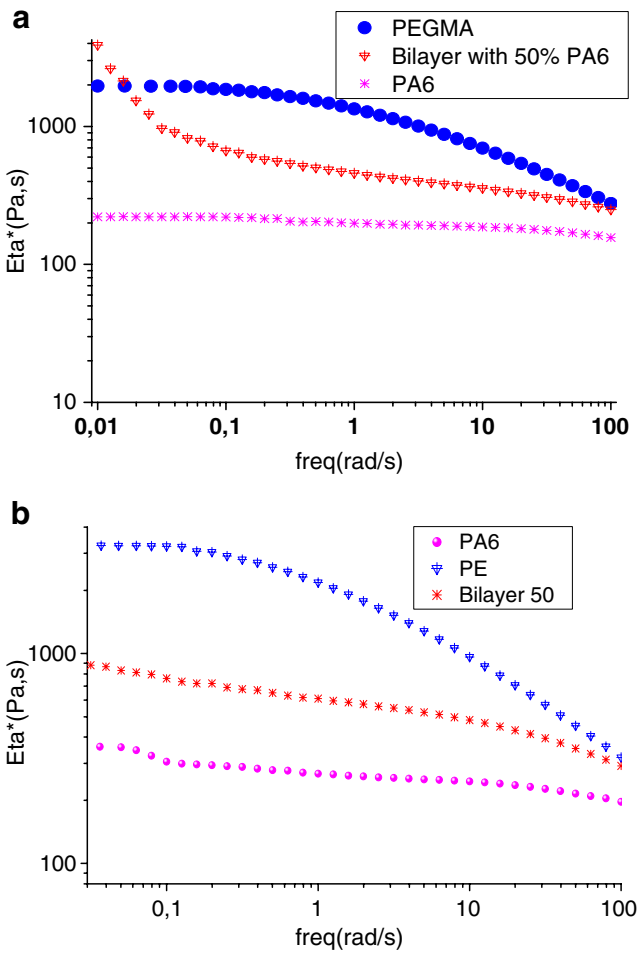

Fig. 1 The viscosity vs the angular frequency at 240 °C for **a** a reactive PE-GMA/PA6 bilayer system (with 50 vol% PA6) and its respective neat components and **b** a nonreactive PE/PA6 bilayer system (with 50 vol% PA6) and its respective neat components

The occurrence of these reactions was confirmed in our previous work (Lamnawar and Maaouz 2006, 2007a,b) by both rheology and Fourier transform infrared spectroscopy. These results were, in fact, in agreement with the findings of Orr et al. (2001) derived from studies of the different kinetics of the reaction between several pairs of polystyrene functional group pairs.

The following reaction in our systems should be controlled by the diffusion rate of the COOH and NH_2 end groups of PA6, as (1) PE-GMA presented more reactive groups (~12.5 GMA functional groups) than the PA6 chain, (2) the reaction temperature (240 °C) was above the glass temperature of PE-GMA, allowing the PE-GMA chains to have a relatively high mobility rate (Lamnawar and Maazouz 2007b; Wei et al. 2005), and (3) the low molecular weight PA6 chain easily adopted a low-entropy, stretched configuration, thus entering into the dense copolymer at the polymer/polymer interface. When changes occur in the density of the reactive groups in the interfacial region and the COOH and NH_2 groups of PA6 experience less reaction opportunities than the GMA groups of the PE-GMA layer, the following reaction should be less diffusion controlled when the interphase become more saturated with in situ formed copolymer (Coote et al. 2003; Yokoyama and Kramer 2000; Harton et al. 2005).

Figure 2 describes a comparison between the rheological behavior of reactive PE-GMA/PA6 bilayer systems with 50 and 30 vol% PA6 and that of the neat components. Both bilayer systems displayed an increase in dynamic viscosity in the lower frequency, which was similar to what was observed in Fig. 1. Meanwhile, the flow curves of the bilayer systems lay between those of the pure polymers for both compositions. More particularly, the flow curves at low angular frequency were higher than for PE-GMA and PE. The increase in the amount of PA6 decreased the viscosity at different shear rates. This phenomenon can be explained by the lower viscosity of PA6. The following expression was obtained from the model of Lin (1979):

$$\eta_{\text{multilayer}} = \frac{\eta_1\eta_2}{\phi_1\eta_2 + \phi_2\eta_1} = \frac{\eta_1\eta_2}{(1-\phi_2)\eta_2 + \phi_2\eta_1} \quad (4)$$

When ϕ_2 increases, the apparent viscosity of the multilayer system decreases again.

Morphology of equivalent blends

Morphological observations were carried out to evaluate the average interfacial area generated with the various strategies of mixing. SEM micrographs and histograms of the size distribution of the blends are shown in Figs. 3 and 4, respectively. The non-reactive blend with a PE matrix (Fig. 3a,b) demonstrates a typical morphology for an incompatible system with the appearance of sharp dispersed particles (D_n=1.4±0.3 μm) and a discrete interface between

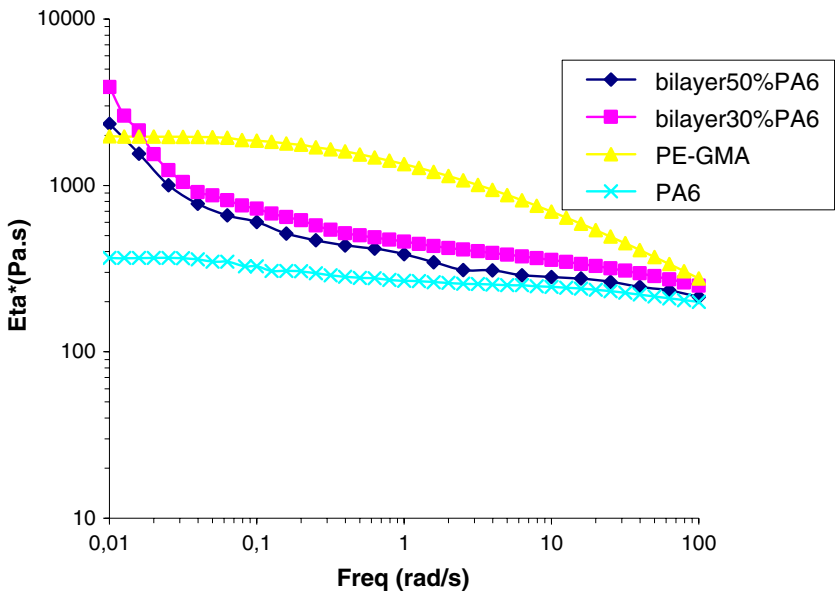

Fig. 2 The viscosity vs the angular frequency at 240 °C for reactive PE-GMA/PA6 bilayer systems with 50 and 30 vol% PA6 as well as for the neat components

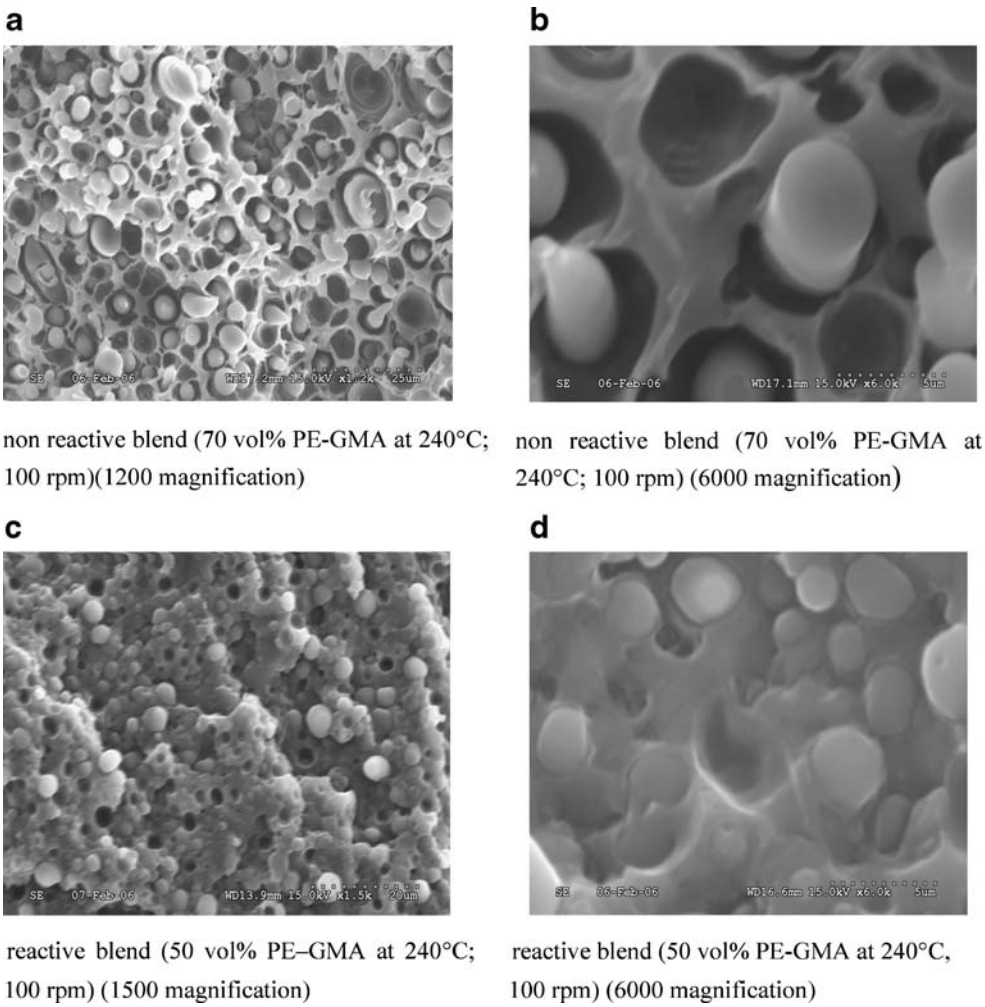

non reactive blend (70 vol% PE-GMA at 240°C; 100 rpm)(1200 magnification)

non reactive blend (70 vol% PE-GMA at 240°C; 100 rpm) (6000 magnification)

reactive blend (50 vol% PE–GMA at 240°C; 100 rpm) (1500 magnification)

reactive blend (50 vol% PE-GMA at 240°C, 100 rpm) (6000 magnification)

Fig. 3 SEM micrographs of **a** and **b** non reactive blends of 70 vol% PE-GMA at 1,500 and ×6,000 magnification, respectively, and **c** and **d** reactive blends of 50 vol% PE-GMA at 1,500 and ×6,000 magnification, respectively. The die temperature was 240 °C and the screw speed 100 rpm

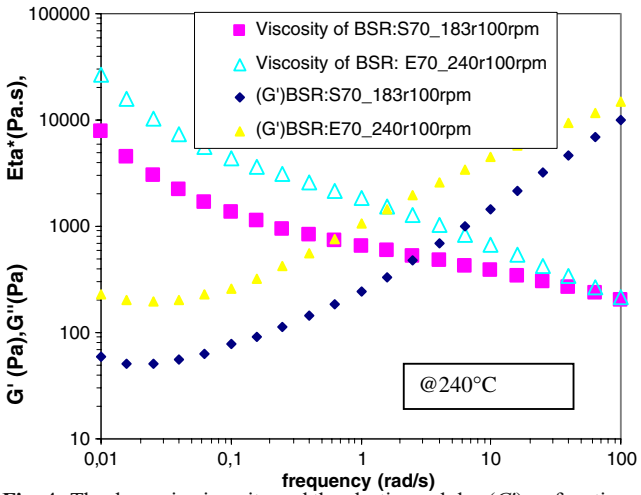

Fig. 4 The dynamic viscosity and the elastic modulus (G') as functions of the angular frequency at 240 °C for emulsion and suspension blends (respectively labeled E70_240r100 and S70_183r100)

the phases due to poor interfacial adhesion. Furthermore, two effects of the reactivity at the interface can be observed: The size of the dispersed phase was significantly reduced (D_n=0.7±0.15 μm) and the droplet size distribution became narrow with enhancement of the adhesion (Fig. 3c,d).

Influence of blending parameters on the viscoelastic properties of the emulsion and suspension mixtures

Figure 4 shows one example of the viscosity evolution vs angular frequency for reactive blends with 70 vol% PE-GMA prepared in the twin screw extruder at 183 and 240 °C and a screw speed of 100 rpm. In this study, the measuring temperature was 240°C, at which the two blends were in the emulsion state. A large difference between suspension/emulsion behavior can be observed. Furthermore, at lower frequencies, the difference was more apparent due to a relaxation phenomenon. The viscosity of a suspension in the emulsion state in the rheometer was lower than its emulsion equivalents for all samples. This gives rise to a question that needs to be considered: How can rheology and interfacial property contributions explain this behavior?

Multilayer systems: effect of interfacial area in interdiffusion/reaction phenomena

Multilayers as model systems to study polymer blending and to probe interdiffusion/reaction phenomena

Manually prepared multilayers of cast films or hot-pressed films of a pair of reactive compatible polymers have been used by several researchers to study interfacial reactions (Saito and Macosko 2002). In these layered structures, the interfacial area is clearly defined and remains constant. The overall interfacial reaction rate is only determined by the intrinsic reaction rate and the diffusion rate, and the rheological properties have no effect on the reaction rate measurements. The polymer–polymer interdiffusion can be studied independently by many other means.

The concentration of functional groups is normally low in most reactive blends; a large interfacial area is required to be able to measure a reaction. In a multilayer sample, the area of one interface is limited, but by utilizing a large number of layers, one can generate a large interfacial area. In the cast film technique, the number of layers is limited to several layers. In the present study, multilayer samples obtained through coextrusion presented interfacial areas sufficiently large to allow reliable measurements of interfacial reaction by rheological tests.

For this purpose, multilayer samples of PE-GMA/PA6 with a varying number of layers were annealed in the parallel plate rheometer at 240 °C. Figure 5 describes the results of frequency sweep experiments for a reactive multilayer with 70 vol% PE-GMA and varying numbers of layers/interfaces and compares them with the equivalent suspension and emulsion based systems (S70, T183; S70, T240) prepared at 240 °C and a screw speed of 100 rpm. In addition, typical changes in the viscosities for these multilayer systems vs the healing time, at the same temperature, are presented in Fig. 6 for 1 rad/s.

Referring to Figs. 5 and 6, the multilayer viscosities showed significant increases with increasing interfacial areas. In other words, increasing the number of interphases also increased the viscosity moduli. The results displayed that, as a consequence, the variation in viscosity of the multilayer system reflected the occurrence of both diffusion and chemical reaction: Because of the increase in interface adhesion strength due to the coupling reactions between epoxy, carboxylic, and amino groups, interdiffusion phenomena were found to increase when the kinetics of the chemical reaction at the interfaces also improved. Indeed, the interfacial reaction could only occur when PA6 and PE-GMA chain ends were able to penetrate through each layer and the copolymer interphase to meet the antagonist reactive functions at the interface. Obviously, the diffusion rate of PA6 through the bulk layer was different from the one through the copolymer layer. The former was obtained through self-diffusion in the same phase, whereas the latter was dependent on the penetration rate through the interphase, which should be much slower than the self-diffusion due to the denseness of the copolymer barrier. Moreover, the rheological behavior of the suspension blend studied at 240 °C in its molten state seemed to be very close to that of its equivalent in a multilayer system with a large number of layers. Meanwhile, a clear relationship between viscoelastic material functions of multilayer systems and compositions

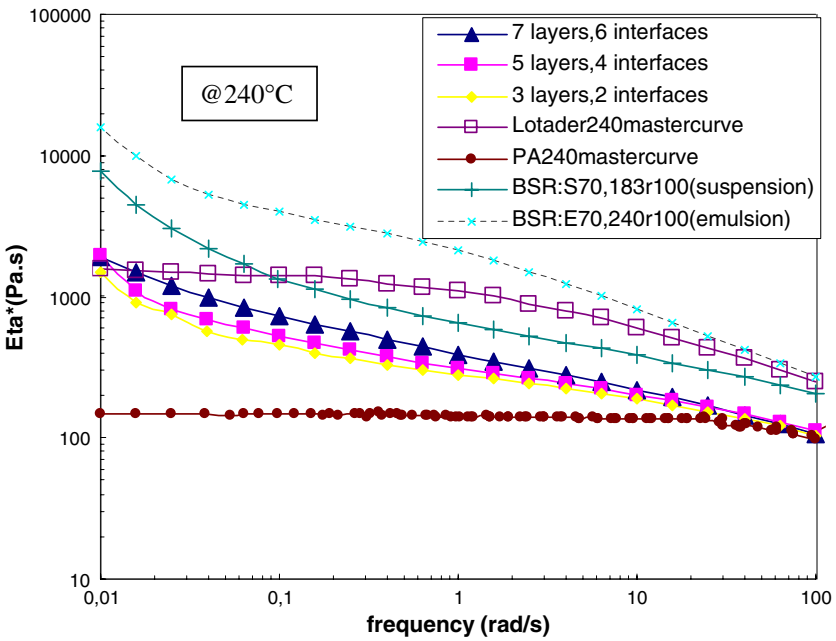

Fig. 5 The viscosity vs the angular frequency at 240 °C for reactive multilayers with 70 vol% PE-GMA and varying numbers of layers/interfaces as well as the corresponding curves for their equivalent suspension- and emulsion-based systems

can be evaluated to analyze the effect of bulk and reactive functions in the polyolefin phase at the interface with PA.

On the other hand, the complex viscosity of the melt system with 30 vol% PA6 was taken from Fig. 6 and plotted in Fig. 7. Indeed, the logarithm of the viscosity value at 100 rad/s as a function of the volume fraction of the PE phase is reported in this paper. The frequency was chosen based on the observed closed behavior of multiphase systems and their components. Naturally, the use of the corresponding viscosity values from the plot vs the composition can be considered only in a phenomenological way to fit model equations. Indeed, the rheological results were rationalized by comparing the obtained data with some existing theoretical models. Good agreement with the reciprocal rule was observed for multilayer systems, while a positive deviation was found for both suspension and emulsion reactive blends.

Quantification of interfacial area effect

Figure 8 shows the viscosity evolution of both multilayer and blend systems vs the interfacial area at 10 and 100 rad/s. Indeed, the intersection between the viscosity evolution of the multilayer (vs the number of layers in the sandwich where $\pi R^2=\pi\ (12.5)^2$ represents a surface of each layer) with the viscosity of the equivalent blend at a given volume fraction allow the extrapolation of this point to the axis of the interfacial area (given number of layer=interfacial area/

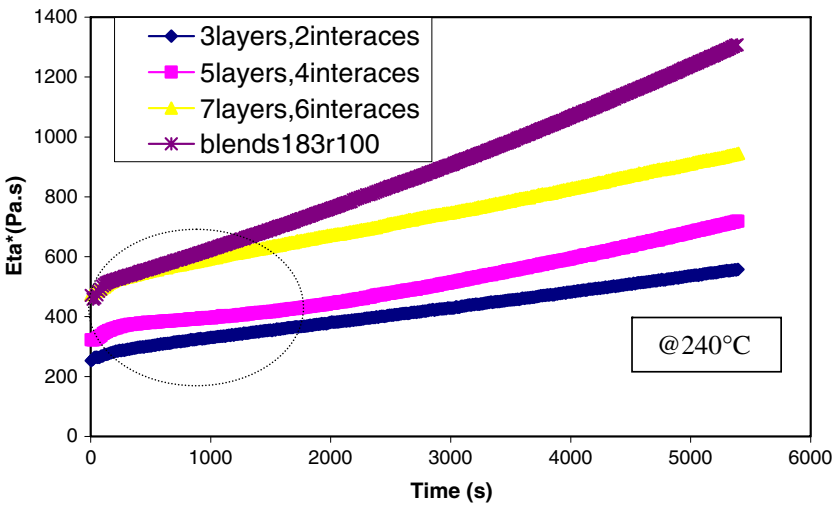

Fig. 6 The viscosity vs the healing time at 240 °C at a given frequency of 1 rad/s for reactive multilayers with 70 vol % PE-GMA and varying numbers of interfaces

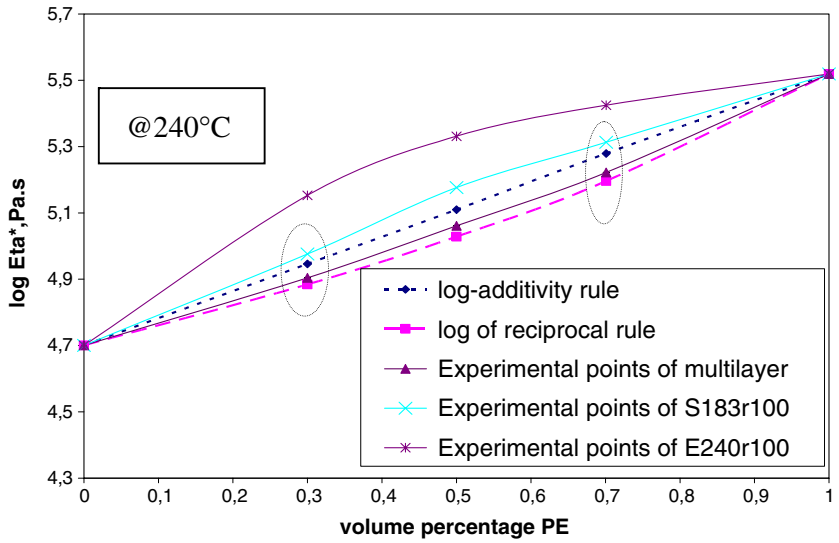

Fig. 7 The viscosity as a function of volume percentage for a PE-GMA multilayer system (seven layers, six interfaces), as well as for a reactive suspension and emulsion of equivalent blends measured at 100 rad/s. These curves are compared with existing models of multiphase systems

$\pi R^2 = \pi\ (12.5)^2$). Hence, the equivalent interfacial area of the blend can be evaluated. The results demonstrate the possibility of quantifying the equivalent interfacial blend area by studying multilayer structure at varying shear rates and decoupling rheology/interfacial properties.

From dimensional considerations, it was shown (Fig. 8) that an n-multilayer system was equivalent to an emulsion system of inclusions of a given size in a blend.

Solubility tests in formic acid, which is a good solvent for PA, demonstrated that polyethylene constituted the matrix in both compositions. For a fixed blend composition, the compatibilization reaction can be largely affected by the processing conditions. The suspension-type mixture (Fig. 9a) displayed a morphology typical of immiscible blends, with the appearance of sharp dispersed particles (mean diameter $D_n = 150 \pm 50$ μm) and a discrete interface between the two phases. This was due to a poor interfacial adhesion. In this case, the extruded blend was prepared at a temperature of 183 °C at which the dispersed PA6 phase was solid and the matrix was molten. For the emulsion-type blends prepared at 240 °C, on the other hand, two reactivity effects could be observed at the interface: The size of the

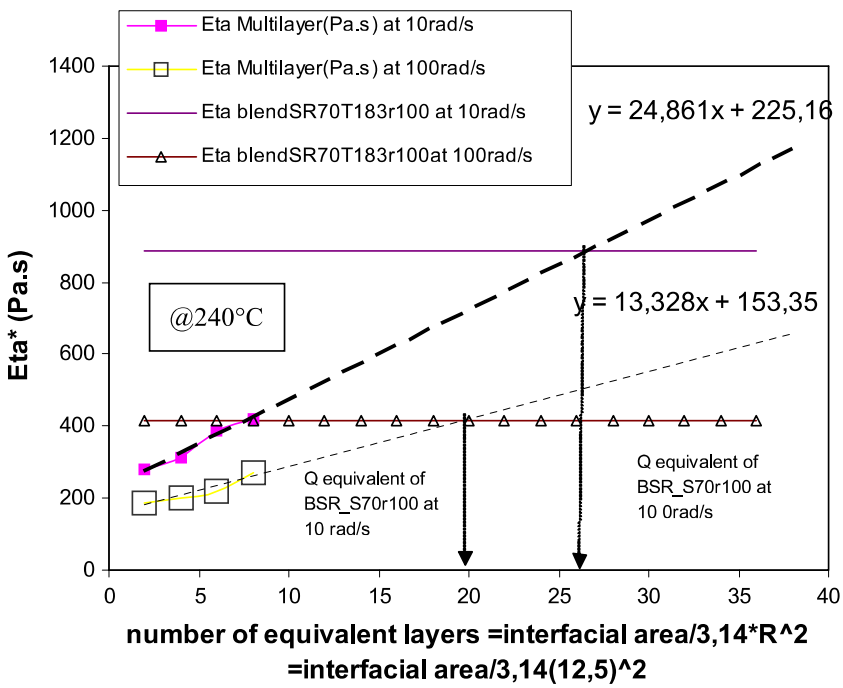

Fig. 8 The viscosity evolution of both multilayer and blend systems vs. the interfacial area at 10 and 100 rad/s

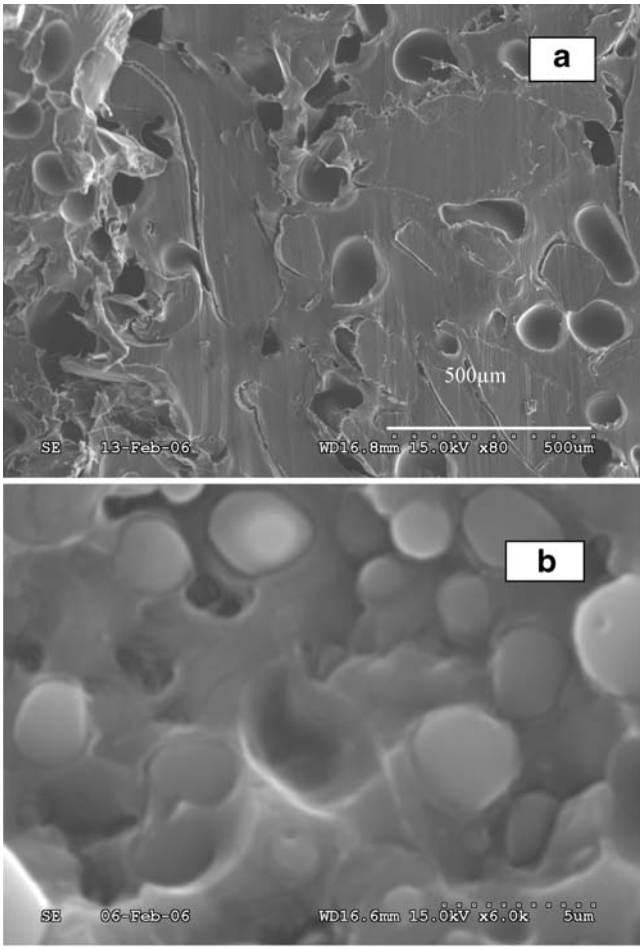

Fig. 9 SEM micrographs of **a** blends with 30% wt of PA6 prepared at 183 °C and a screw speed of 100 rpm for the suspension-type mixture, and **b** a reactive blend (emulsion) prepared at 240 °C demonstrating the fixed droplet morphology after rheological measurements

dispersed phase was significantly reduced and the adhesion was enhanced. A comparison between the two processes indicated a significant compatibilizing effect in the case of the emulsion type, which can be explained by a larger number of opportunities for interfacial reactions when the two components were in their molten states. A higher amount of interfacial reactions led, in turn, to decreases in the interfacial tension and in the coalescence process. In the case of a reactive emulsion system, at high temperatures and after rheological measurements, less rupture of droplets could be obtained since the interphase was created.

Indeed, it should be noticed that this size depends on the approach used to obtain the samples: For a blend in which the inclusions are kept in a solid state (i.e., suspension) the necessary number of layers to obtain an equivalent behavior must be lower than when the inclusions were melted before the rheometry trials. This difference depended on the shear applied in the rheological experiments. The emulsion-based system had an inclusion size that did not change from the initial state. An exception was the relaxation of droplets, as the interphase that was created before the rheological test presented no rupture of these droplets (fixed cross-linking system, Fig. 9b). In the suspension-based system, the interfacial reaction amount was very small. The droplet could relax and separate before the interphase creation. The shear influence was therefore obvious: At a low shear rate, the emulsion-based (E) and suspension-based (S) systems showed different rheological behavior, but once increased, they tended to strive towards a similar one. Indeed, the equivalence between a multilayer and a blend is influenced by the approach for obtaining the emulsion and the shear rate. The interfacial areas obtained by extrapolation were 9.81×10^{9} µm^2 ($\omega=10$ rad/s) and 1.22×10^{10} µm^2 ($w=100$ rad/s). The equivalent values/unit volume: $Q/\text{volume} = n\pi(R)^2 \Big/ H*\pi(R)^2 = {}^{n}/_{H}$ are given in Table 3 where the comparison between the theoretical values is also presented.

Evaluation of the interphase effect by thermodynamical tool

General aspects

The interaction between two polymers can be investigated by measuring the interfacial thickness. The interface between polymer/polymer pairs is not very thick and is typically on the order of 2 to 50 nm depending on the nature of the interaction. When two films of miscible polymer pairs are brought together and heated above their *T*g, a broad interface develops with time. Immiscible systems, on the other hand, give rise to thin interfaces; this situation is schematically shown in the literature (Wool

Table 3 Equivalent interfacial area per unit volume for multilayer and blend systems

Blend/composition	D_n (µm)	Interfacial area/unit volume (µm^{-1}): $A_i = \frac{3\alpha}{R}$	Experimental interfacial area evaluated by rheological method/unit volume (µm^{-1})
BSR 70: S183 r100 Studied at 240 °C	126	14.28×10^{-3}	16.66×10^{-3} ($\omega=10$ rad/s) 22.03×10^{-3} ($\omega=100$ rad/s
BSR70: E240 °C r100 Studied at 240 °C	1.19	1.51	–

1995). If two polymers are strongly immiscible, their chains repel each other, and the penetration of each chain end from either phase into the other across the interface is highly unfavorable. In such a case, the interfacial tension is high and the interfacial thickness small. For immiscible systems, both mean-field and lattice theories predict that some interdiffusion of polymer segments occurs at the interface to minimize the interfacial energy. It is postulated that the thickness of the interface is proportional to $\chi^{-0.5}$, while the interfacial tension behavior of both polymers is proportional to $\chi^{-0.5}$, where χ denotes the Flory–Huggins segmental interaction parameter. Immiscible polymers have a large and positive χ. When using the Flory–Huggins solution theory applied to a binary polymer blend system (Flory 1953), it is possible to find the critical condition for miscibility in such a system in terms of the interaction parameter χ, as

$$\begin{aligned} \chi_{ab} &= V \Big/ RT(\delta_a - \delta_b)^2 \\ \chi_{crit} &= \tfrac{1}{2}\left(\tfrac{1}{\sqrt{N_1}} + \tfrac{1}{\sqrt{N_2}}\right)^2 \end{aligned} \tag{5}$$

In this equation, N is the polymerization degree. The χ_{crit} for the studied NSR and SR with values of N_{PE}=750, $N_{PE\text{-}GMA}$=928 and N_{PA}=150 was 0.00698 and 0.0065, respectively. δ is the solubility parameter expressed in units of $J^{1/2}/cm^{2/3}$, V is the molar volume (cm^3/mol), R is the gas constant (cal/mol k), and T is the absolute temperature (K).

In thermodynamics of polymers (Helfand and Tagami 1972; Joanny and Leibler 1978; Wool 1995), two-component systems recognize two terms: interface and interphase. The thickness of the interphase, Δl (on the order of the mean gyration radius of the components), is inversely proportional to the interfacial tension coefficient α_{12}:

$$\begin{aligned} &\Delta l = [(2k_BT)/9b][(\chi - \chi_{crit})/\chi_{crit}]/\alpha_{12} \\ &\text{with}: \chi = \tfrac{V}{RT}(\delta_a - \delta_b)^2 \\ &\text{and}: \chi_{crit} = \tfrac{1}{2}\left(\tfrac{1}{\sqrt{N_1}} + \tfrac{1}{\sqrt{N_2}}\right)^2 \end{aligned} \tag{6}$$

where b_i is the effective bond length of a statistical segment in the melt, with typical values in the range 5–7 Å.

The average interfacial width is related to the thermodynamic interactions and can be estimated from the relation derived by Helfand and Tagami. On the basis of these equations (Eq. 6), Todd et al. (2003) have calculated the interfacial widths using functionalized bilayer systems as anhydride terminal poly(methyl methacrylate) and polystyrene with amine-functional polystyrene.

Estimation of interfacial tension of RS and NRS

According to the work of Deyrail (2002) and with reference to the Taylor theory, measurements of interfacial tension were carried out on a PE/PA6 blend by the drop retraction method. This is a classic method employed by several others. By using the Linkam device, a step deformation was imposed to a melt drop of PA6 imbedded in a molten PE matrix. The relaxation process was then optically recorded until the drop returned from an ellipsoidal to an equilibrium spherical shape. Subsequently, as the viscosity of both components was known, the interfacial tension could be inferred from dimensional variations of the deformed drop as a function the relaxation time. Such an experiment was carried out on different droplets so as to obtain reproducible values of the interfacial tension. The various PA6 droplets were obtained from a fine PA6 powder dispersed between two circular PE or PE-GMA films, with thicknesses of about 500 μm. To obtain well-defined spherical droplets, the dispersed particles were subjected to a shear treatment during a determined time (30 s; steady shear 1 s^{-1}), thus giving rise to short filaments of PA6. The flow was then stopped and the filaments were allowed to retract and to break into smaller domains.

Referring to Taylor's theory, it is known that the recovery of a deformed viscous drop, immersed in a second fluid submitted to shear treatment at small amplitudes of deformation, is driven only by interfacial tension. Moreover, the rheological properties of the polymer do not change during the recovery process.

For clarity purposes, the calculation method can be found in the annexe.

The experimental results and corresponding linear fits (Lamnawar and Maazouz 2007b) give us access to the value of interfacial tension for the studied blend. Thus, it was found that the interfacial tension value decreased from 5.25 mN/m in a nonreactive system to 0.17 mN/m in a reactive one.

As a consequence, an interphase thickness of 6 Å was found in the case of the nonreactive system and of 20 nm for the reactive one, at 240 °C using Eq. 6. These results corroborate those of Yukioka and Inoue (1993) and Abdellah and Utracki (1996).

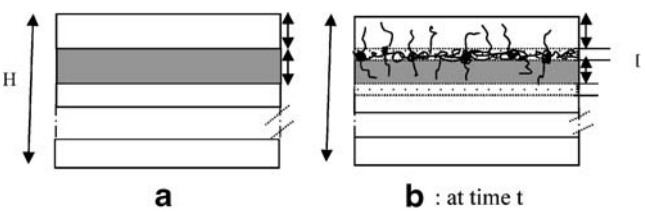

Fig. 10 A schematic of the interface/interphase geometry at **a** time t_0 and **b** time t

Evaluation of the interphase effect by rheological tool

When a multilayer sample is sheared in parallel plates, the stress across each layer is the same, and the total strain is the sum of the strain of each layer (Lin and Chang 1991). The situation of interest is pictured in Fig. 10. Indeed, at the initial state (Fig. 10a), the apparent complex viscosity η^*_{SR} is given by a relationship between the component viscosity and volume fraction of the sandwich structure Bousmina et al. (1999):

$$\frac{1}{\left(\eta^*_{SR}\right)_{t=0}} = \sum^{i} \frac{\phi_{a,i}}{\eta^*_{a,i}} + \sum^{j} \frac{\phi_{b,j}}{\eta^*_{b,j}} = \sum^{i} \frac{h_{a,i}/H}{\eta^*_{a,i}} + \sum^{j} \frac{h_{b,j}/H}{\eta^*_{b,j}} \tag{7}$$

where η^*_{SR}, $\eta^*_{a,i}$ and $\eta^*_{b,j}$ denote the viscosities of a multilayer system and of layers a and b. The parameters $h_{a,i}$ and $h_{b,j}$ reperesent the thicknesses of each layer and H, the total layer thickness. ϕ_i is the volume fraction of each component and is given by h_i/H. $\phi_a + \phi_b = n_a h_a/H + n_b h_b/H = 1$.

However, the prediction according to Eq. 7 is only valid with very short reaction times where the interface between two neighboring layers is very small and flat. Indeed, as the reaction and mutual diffusion proceed, the interface strengthens, giving rise to an interphase with its own thickness and rheological properties, and the viscosity of the multilayer system is controlled by each of its layers and especially by the developed interphase (Fig. 10b). Furthermore, the interface generated due to chemical reactions between the carboxylic acid and amino groups at the chain end of PA6 and the epoxy groups in PE-GMA becomes roughened. This roughened interface would cause an additional friction against the flow near the interface, which would increase the viscosity. Hence, the interphase consisted of PE-GMA-copolymer-PA6, and its strength would be much greater than that of an interphase formed strictly from interdiffusion without reaction at the polymer–polymer interface.

The apparent viscosity of a multilayer at time (t) can be related to the viscosity and layer thickness of each component and the present interphase as:

$$\begin{aligned}\frac{1}{\left(\eta^*_{SR}\right)} &= \sum^{i} \frac{\phi'_{a,i}(t)}{\eta^*_{a,i}} + \sum^{j} \frac{\phi'_{b,j}(t)}{\eta^*_{b,j}} + \sum^{i+j-1} \frac{\phi_I(t)}{\eta^*_I} \\ &= \frac{n_a\left[h_a - h_I(t)\left(1 - \frac{1}{n_a+n_b}\right)\right]\Big/H}{\eta^*_a} \\ &\quad + \frac{n_b\left[h_b - h_I(t)\left(1 - \frac{1}{n_a+n_b}\right)\right]\Big/H}{\eta^*_b} \\ &\quad + \frac{(n_a + n_b - 1) * h_I(t)]/H}{\eta^*_I}\end{aligned} \tag{8}$$

in which Φ'_i and $\eta^*_i (i = a, b)$ is the new volume fraction and the viscosity of component i, respectively, n_a and n_b are the number of layers of polymer (a) and (b). The interphase thickness is represented by h_I where η^*_I denotes its viscosity. In this case $\phi_a + \phi_b + \phi_I = 1$. Furthermore, $\sum \Phi'_a(t)$ (or $\sum \Phi'_b(t)$) and $\sum \Phi'_I(t)$ are respectively the volume fractions of polymer (a) [or polymer (b)] and the interphase at a given reaction time t.

Notice that $\sum \Phi'_a(t)$ differs from $\sum h_a/H$ but may be expressed by $\left(n_a h_a \Big/ H - \left(1 - \frac{1}{(n_a+n_b)}\right) h_I \Big/ H\right)$, and $\sum \Phi'_I(t) = (n_a + n_b - 1)h_I/H$. This is because the chains of polymer a (or polymer b) in the graft copolymers were assumed to be located at a distance half the thickness of the interphase.

The summation is also equal to 1 with:

$$\begin{aligned}
&n_a\left[h_a - h_I(t)\left(1 - \tfrac{1}{n_a+n_b}\right)\right]\Big/H + n_b\left[h_b - h_I(t)\left(1 - \tfrac{1}{n_a+n_b}\right)\right]\Big/H + (n_a + n_b - 1)h_I(t)]/H = \\
&= 1\Big/H\left[\left(n_a h_a + n_b h_b - n_a h_I(t) + n_a \tfrac{1}{n_a+n_b} h_I(t) - n_b h_I + n_b \tfrac{1}{n_a+n_b} h_I(t) + (n_a + n_b - 1)h_I(t)\right]\right. \\
&= 1\Big/H\left[\left(n_a h_a + n_b h_b + h_I(t)\left(-n_a - n_b + n_a \tfrac{1}{n_a+n_b} + n_b \tfrac{1}{n_a+n_b} + n_a + n_b - 1\right)\right]\right. \\
&= 1/H\left[\left(n_a h_a + n_b h_b + h_I(t)\left(n_a - n_a + n_b - n_b + \tfrac{n_a+n_b}{n_a+n_b} - 1\right)\right]\right. \\
&= 1/H[(n_a h_a + n_b h_b + h_I(t)(0 + 1 - 1)] = n_a h_a/H + n_b h_b/H = \\
&= \phi'_a + \phi'_b + \phi_I = 1
\end{aligned}$$

It is important to note that Eq. 9 (Bousmina et al. 1999; Zhao 2001) has been also used by Kim et al. (2006) in a reactive bilayer system between PS-mCOOH and PMMA-GMA. In their case $n_a=n_b=1$ and Eq. 9 becomes:

$$\frac{1}{(\eta^*_{SR})} = \frac{\phi_{PS-mCOOH(t)}}{\eta_{PS-mCOOH}} + \frac{\phi_{PMMA-GMA(t)}}{\eta_{PMMA-GMA}} + \frac{\phi_{thirdlayer(interphase)}}{\eta_{interphase}} = \frac{\left[h_{PS-mCOOH} - h_{third\,layer}(t)/2\right]/H}{\eta^*_{PS-mCOOH}} + \frac{\left[h_{PMMA} - h_{third\,layer}(t)/2\right]/H}{\eta^*_{PMMA-GMA}} + \frac{h_{third\,layer}(t)/H}{\eta^*_{third\,layer}} \quad (9)$$

From Eq. 9, we can derive the thickness of the present interphase at the specific welding time and frequency (Eq. 11).

$$h_I(t) \propto \frac{\frac{H}{\eta_{SR}(t)} - n_1 h_1/\eta_1 - n_2 h_2/\eta_2}{\left[\frac{n_1+n_2-1}{\eta_{I\infty}+(\eta_{I0}-\eta_{I\infty})e^{-Kt}} - \frac{n_1}{\eta_1}\left(1-\frac{1}{n_1+n_2}\right) - \frac{n_2}{\eta_1}\left(1-\frac{1}{n_1+n_2}\right)\right]} \quad (10)$$

where η_{I0} and $\eta_{I\infty}$ are initial and saturation viscosities of the interphase, respectively. Hence, it becomes possible to evaluate the evolution of the interphase viscosity and its values at $t_{I0}=0$ and $t_{I\infty}$, when the thickness of the interphase is known.

The interfacial thickness of incompatible layers remained very thin indicating their strong immiscibility. This is portrayed in Fig. 11. However, the interfacial reaction produced the in situ copolymers in different ways in reactive system. The interfacial region increased with the healing time and then reached a maximum value of 35 nm, as can be seen in Fig. 12.

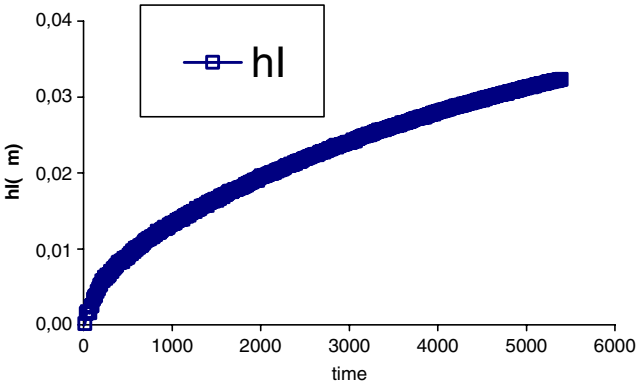

Fig. 12 Example of curve given the interphase thickness evolution as a function of time for **a** a three-layer PE-GMA/PA6/PE-GMA system at 240 °C

To interpret the thick interface of the reactive compatibilization, Koriyama et al. (1999) proposed two plausible models: The first consists in an undulated interface and the other in micelle formation. In the former model, some experiments have already proven that an undulated interface existed after the interfacial reaction. In our example, the interfacial thickness at high welding times was roughly 35 nm (Fig. 12). This was confirmed by both SEM (Fig. 13) and the previously demonstrated thermodynamic evaluation.

A reasonable explanation for the present undulated interface was that the copolymer formation reduced the interfacial tension, as far as to zero, and that the thermal fluctuations during the interfacial reaction could lead to the undulated interface, which could be covered by more copolymers than a flat interface. Another reason that can explain the phenomena refers to the viscosity ratio. Recently, S. Patlazhan et al. (2006) observed, using a level set method of simulation, growth of interface perturbations with the increase of the viscosity ratio. Indeed, for the present

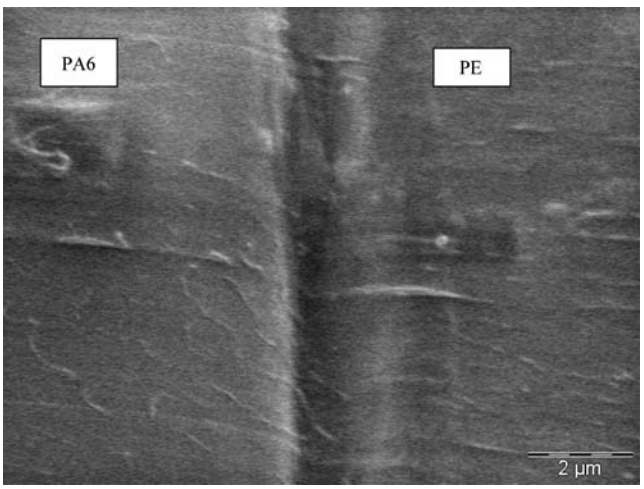

Fig. 11 A SEM micrograph of a sharp interface of the incompatible PE/PA6 bilayer system

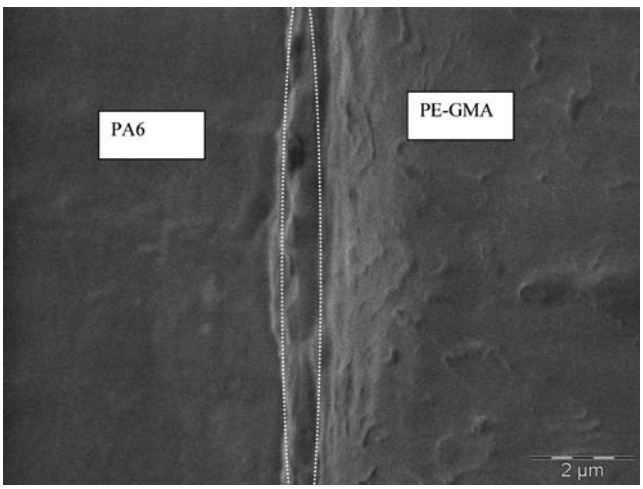

Fig. 13 A SEM micrograph of the interface/interphase of a compatibilized PE-GMA/PA6 bilayer system

experiment (under a small shear flow=1 rad/s, T=240 °C), the viscosity ratio $m = \eta_{PE}/\eta_{PA6(1)}$ was 5 (Fig. 14). The effect can be illustrated by a local pressure gradient, which can develop in the vicinity of the interface despite the fact that the global flow was a simple shear. This effect gave rise to the present instability, which led to interface disturbances with processing time. Moreover, it can be seen that larger amounts of viscous fluid were extended to a less viscous layer (Fig. 15).This was explained by the fact that the pressure that developed in a more viscous layer was higher than that in one with a lower viscosity.

Work in progress

A way to evaluate the different appearing morphology generated at the interface/interphase by AFM and TEM tools is in progress.

Concluding remarks

In the present study, the effect of the interfacial area on the viscoelastic properties of multilayer functionalized polymers was investigated. A significant influence on the existence of interfacial reactions and interfacial morphologies was demonstrated. Indeed, the shear amplitude was found to help enhance the extent of chemical reactions/interdiffusion at the polymer/polymer interface with the generation of an interphase, as long as its magnitude was small. The same phenomena could be observed when increasing the temperature and contact time.

Dynamic mechanical experiments were performed to probe the effect of the interfacial area on the rheological behavior of the multilayered structure and compare it to that of a droplet-type morphology. PA6/PE-GMA was used as a model system. In its molten state, such a system generated a reaction between amine, carboxylic, and epoxy groups. Multilayer structures containing various amounts of both interfacial area and volume fractions were studied. Relationships between viscoelastic material functions and compositions were used to analyze the effect of bulk and reactive functions in the polyolefin phase at the interface with PA. The number of layers was varied to increase the contribution effect of the interface/interphase. The results showed that the variation in dynamic modulus of the multilayer system was a result of both diffusion and chemical reaction. Specific experiments were carried out to separate the thermodynamic effects from the kinetic ones. The results were rationalized by comparing the obtained data with theoretical models. Finally, to quantify the contribution effect of the interface/interphase with a specific interfacial area, an expression was developed taking into account the interphase triggered between the neighboring layers at a specific welding time and shear rate. The experimental results were in good agreement with the theoretical ones.

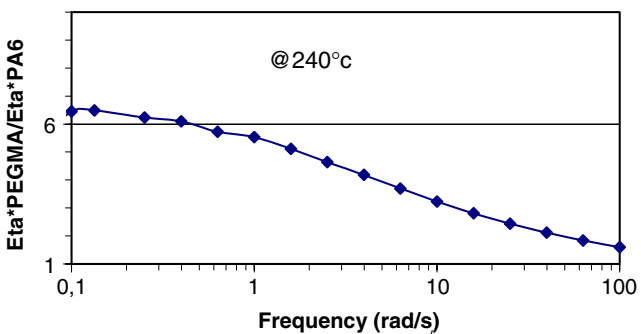

Fig. 14 The evolution of viscosity $m = \eta_{PE}/\eta_{PA6}$ as a function of frequency at 240 °C

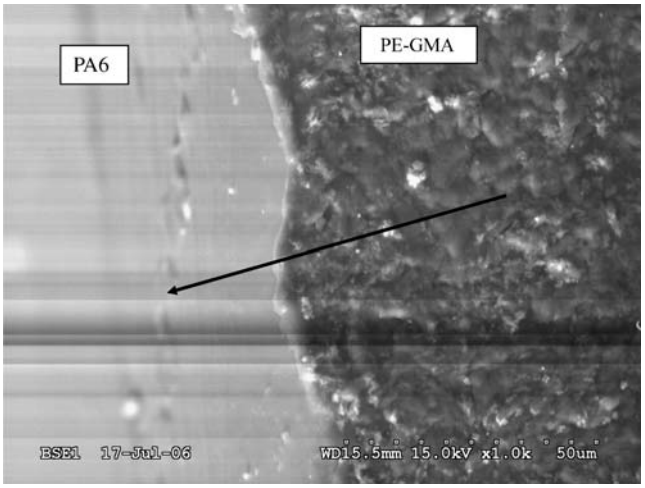

Fig. 15 A SEM micrograph of the undulated interface of a PA6/PE-GMA bilayer system

Acknowledgements The authors wish to thank ARKEMA for providing the PE-GMA and PE and BASF for providing the PA6 sample. Mr. Alain Roche from "CNRS/Laboratoire des Matériaux macromoleculaires Lyon 1" is acknowledged post-mortem (died on October 9, 2005) for assistance and fruitful discussions.

Annexe

The calculation method of interfacial tension is based on the following expression of the deformation D toward the equilibrium shape of the droplet

$$D = D_0 \exp\left\{-\frac{40(p+1)}{(2p+3)(19p+16)}\frac{\alpha_{12}}{\eta_m R_0}\right\} = D_0 \exp\left\{-\frac{t}{\tau_d}\right\} = \frac{L-B}{L+B}$$

In this equation, D_0 is the deformability parameter at the initial time, p is the viscosity ratio, L and B represent respectively the major and minor axes of the ellipsoid, and

α_{12} is the interfacial tension. τ_d is the relaxation time according to:

$$\tau_d = \frac{\eta_{eq} R_0}{\alpha_{12}}$$

and η_{eq} is the equivalent viscosity

$$\eta_{eq} = \frac{(2p+3)(19p+16)\eta_m}{40(p+1)}$$

The results and corresponding linear fits [Ln $(D)=f(t)$], give us access to the value of interfacial tension for studied systems [PE-GMA/PA6(RS) and PE/PA6 (NRS)].

References

Abdellah A, Utracki LA (1996) Interphase and compatibilization of polymer blends. Polym Eng Sci 36(12):1574–1585

Baker M, Scott C, Hu G-H (2001) Reactive polymer blending. Hanser, Munich

Bousmina M, Palierne J-F, Utracki LA (1999) Modeling of structured polyblend flow in a laminar shear field. Polym Eng Sci 39:1049–1059

Coote ML, Gordon DH, Hutchings LR, Richards RW (2003) Neutron reflectometry investigation of polymer–polymer reactions at the interface between immiscible polymers. Polymer 44:7689–7700

Deyrail Y, Fulchiron R, Cassagnau P (2002) Morphology development in immiscible polymer blends during crystallization of the dispersed phase under shear flow. Polymer 43:3311–3321

Fan X, Chixing Z, Wei Y, Defeng W (2005) Reaction kinetics study of asymmetric polymer-polymer interface. Polymer 46:8410–8410

Flory PJ (1953) Principles of polymer chemistry. Cornell University Press, Ithaca, NY

Fredrickson GH, Scott Milner T (1996) Time-dependent reactive coupling at polymer-polymer interfaces. Macromolecules 29:7386–7390

Harton SE, Stevie FA, Ade H (2005) Diffusion-controlled reactive coupling at polymer-polymer interfaces. Macromolecules 9(38):3543–3546

Helfand E, Tagami (1972) The theory of the interface between immiscible polymers. II. J Chem Phys 56:3592–3601

Jiao J, Kramer EJ, de Vos S, Moller M, Koning C (1999) Morphological changes of a molten polymer/polymer interface driven by grafting. Macromolecules 32:6261–6269

Joanny JF, Leibler LJ (1978) Effects of polymer solutions in colloid stability. J Phys (Paris) 39:951

Kim HY, Jeong U, Kim J-K (2003) Reaction kinetics and morphological changes of reactive polymer-polymer interface. Macromolecules 36:1594–1602

Kim JB, Kang H, Char K, Katsow K, Fredrikson GH, Kramer E (2005) Interfacial roughening induced by the reaction of end-functionalized polymers at a PS/P2VP interface: quantitative analysis by DSIMS. Macromolecules 38:6106–6114

Kim HY, Kim H-J, Kim JK (2006) Effect of interfacial reaction and morphology on rheological properties of reactive bilayer. Polym J 38:1165–1172

Koriyama H, Oyama HT, Ougizawa T, Inoue T, Weber M, Koch E (1999) Studies on the reactive polysulfone-polyamide in interfacial thickness and adhesion. Polymer 40:6381

Lamnawar K, Maazouz A (2006) Rheological study of multilayer functionalized polymers: Characterization of interdiffusion and reaction at polymer/polymer interface. Rheol Acta 45:411–424

Lamnawar K, Maazouz A (2007a) Reactive functionalized multilayer polymers in coextrusion process. Mater Sci AIP Conf Proc 907:908–914

Lamnawar K, Maazouz A (2007b) Interfacial rheology of multilayer functionalized polymers. Mat & Techniques 5(94):305–322

Lin CC (1979) A mathematical model for viscosity in capillary extrusion of two-component polyblends. Polym J 11:185–192

Lin KK, Chang DH (1991) Polymer-polymer interdiffusion during coextrusion. Polym Eng Sci 31(4):258–268

Lyu SP, Cernohous JJ, Bates FS, Macosko CW (1999) Interfacial reaction induced roughening in polymer blends. Macromolecules 32:106–110

Orr CA, Cernohous JJ, Guegan P, Hirao A, Jeon HK, Macosko CW (2001) Homogeneous reactive coupling of terminally functional polymers. Polymer 42:8171–8178

O'Shaughnessy B, Vavylonis D (1999) Reactive polymer interfaces: how reaction kinetics depend on reactivity and density of chemical group Macromolecules 32:1785–1796

Patlazhan S, Schlatter G, Serra C, Bouquey M, Muller R (2006) Shear-induced fractal morphology of immiscible reactive polymer blends. Polymer 47:6099–6106

Prochazka F, Majesté JC, Dima R, Carrot C (2004) Experimental and theoretical description of low frequency viscoelastic behaviour in immiscible polymer blends. Polymer 45:4095–4104

Saito T, Macosko CW (2002) Interfacial crosslinking and diffusion via extensional rheometry. Polym Eng Sci 42:1–9

Schulze SJ, Jeffrey JC, Hiraro A, Lodge TP, Macosko CW (2000) Reaction kinetics of end-functionalized chains at a polystyrene/poly (methyl methacrylate) interface. Macromolecules 33:1191–1198

Thomas S, Groeninckx G (1999) Reactive compatibilisation of heterogeneous ethylene propylene rubber (EPM)/nylon 6 blends by the addition of compatibiliser precursor. Polymer 40:5799–5819

Todd DJ, Schulze JS, Macosko CW, Lodge TP (2003) Effect of thermodynamic interactions on reactions at polymer/polymer interfaces. Macromolecules 36:7212–7219

Tucker CL, Moldenaers P (2002) Microstructural evolution in polymer blends. Annu Rev Fluid Mech 34:177–210

Utracki LA (2000) Polymer structure and morphology. NATO Sci Ser E 370:3–46

Wei Q, Chionna D, Pracella M (2005) Reactive compatibilization of PA6/LDPE blends with glycidyl methacrylate functionalized polyolefins. Macromol Chem Phys 206:777–786

Wool PR (1995) Polymer interface. In: Structure development at semicrystalline interfaces. Hansers, Munich, p 383

Xiaobo Y, Yang W, Binyao L, Yanchun H (2005) Studies on interfacial reaction kinetics and properties at a reactive compatibilization interface. Polymer 46:3337–3342

Yokoyama H, Kramer EJ (2000) Mutual diffusion of asymmetric block copolymers with homopolymers. Macromolecules 33:1871–1877

Yu W, Bousmina M, Gremla M, Palierne J-F, Zhou C (2002) Quantitative relationship between rheology and morphology in emulsions. J Rheol 46:1381–1399

Yukioka S, Inoue T (1993) Ellipsometric studies on immiscible polymer-polymer interfaces. Polymer 3(4):1256–1259

Zhang J, Lodge TP, Macosko CW (2005) Interfacial morphology development during PS/PMMA reactive coupling. Macromolecules 38:6586–6591

Zhao R (2001) Multilayer coextrusion reveals interfacial dynamics in polymer blending. Ph.D. thesis, University of Minnesota